IEEE Access
Multidisciplinary | Rapid Review | Open Access Journal

Received November 7, 2019, accepted November 17, 2019, date of publication November 20, 2019, date of current version December 4, 2019.

Digital Object Identifier 10.1109/ACCESS.2019.2954587

Broccoli Seedling Segmentation Based on Support Vector Machine Combined With Color Texture Features

KUNLIN ZOU, LUZHEN GE, CHUNLONG ZHANG, TING YUAN, AND WEI LI
College of Engineering, China Agricultural University, Beijing 100083, China

Corresponding author: Chunlong Zhang (zcl1515@cau.edu.cn)

This work was supported in part by the National Natural Science Foundation of China under Grant 31601217, and in part by the National Science and Technology Support Program under Grant 2015BAF20B02.

ABSTRACT The segmentation of broccoli seedlings in the crops and weeds co-exist field environment is of great significance for weeding and herbicide spraying. This paper constructed a crop segmentation algorithm with a small training set for discriminating broccoli seedlings from weeds and soil. This algorithm was based on a support vector machine (SVM) combined with color-texture features. Correlation analysis and chi-square tests were used to select 6 features from the 21 color features. Gray-level co-occurrence matrix (GLCM) was used to extract 5 texture features. And each parameter of GLCM had been assessed and optimized by the chi-square test. Linear Discriminant Analysis (LDA) was used to decompose the original dataset in a set of 3 successive orthogonal components. This method selected features more reasonable and gained higher plant segmentation accuracy. When the training sample is greater than 50, the accuracy of the test set could reach 90%. The coefficient of determination (R^2) between the ground truth broccoli seedling area and the segmentation broccoli area was 0.91, and the root-mean-square error (σ) was 0.10. Results demonstrated that the color-texture features were able to effectively segment broccoli seedlings even when there was a significant amount of weeds.

INDEX TERMS Pattern recognition, multiple features, support vector machine, broccoli seedling, weed.

I. INTRODUCTION

Broccoli is one of the most important vegetable plants in the world [1]. Cauliflowers and broccoli were 12th in the world ranking of production of vegetables in 2017 with a production volume of about 26 million tons [2]. Weeds result in a reduction in broccoli yield as the weeds compete with the main crop for space, light, moisture, nutrients [3]. Weed management require huge quantities of herbicides [4]. There are some constraints with chemical weeding such as the high cost of herbicides and harmful effects on the environment and human health [5]. Site-Specific Weed Management is becoming the focus of future farming technologies [6]. The key to precise weeding is to discriminate crop from weeds and soil [7].

In recent years, along with advancements in machine vision systems, several approaches using image processing for weed and crop detection have been investigated [8], [9]. There are certain segmentation methods of crops and weeds mainly based on spectral imaging [9]–[11]. But in the broccoli field, spectral characteristics of crops and weeds are similar. Therefore the feature set for plant recognition has mostly been limited either to multi- or hyper-spectral signatures [12]. Three-dimensional information can be used to identify weeds and crops effectively [13]–[15]. Acquiring 3D under outdoor conditions is limited by the sensor technology and the data processing speed [16]. Deep learning can automatically learn the hierarchical feature expression of images [17]. There are some image segmentation algorithms based on deep learning, such as fully convolutional networks, dilated convolutions, large kernel matters [18]–[20]. Some researchers developed crops segmentation algorithms based on deep learning [21]–[23]. Teimouri *et al.* [24] researched weed growth stage with deep learning. It achieved an average 70% accuracy rate in estimating the number of leaves and 96% accuracy when accepting a deviation of two leaves. The training set of this research was 11,907 images. Huang *et al.* [25] researched a weed mapping method for unmanned aerial vehicle images based on a fully convolutional network. The overall accuracy of the FCN approach was up to 0.94 and the accuracy for weed recognition was 0.88. In their research, each original imagery was divided into

The associate editor coordinating the review of this manuscript and approving it for publication was Jeon Gwanggil.

12 tiles of size 1000 × 1000, and 1092 tiles were obtained in total. Among the whole imagery tiles, 892 titles were randomly selected as training dataset. Ma *et al.* [26] researched an algorithm for rice seedling and weed image segmentation at the seedling stage in paddy fields based on the fully convolutional network, U-Net, and SegNet, respectively. The average accuracy rate of the SegNet method was 92.7%, the average accuracy rates of the FCN and U-Net methods were 89.5% and 70.8%, respectively. In this research, the size of the tiles was 912 × 1024 pixels and the number of tiles was 224. Eighty percent of the samples were randomly selected as the training dataset and 20% of samples were used as the test dataset. Segmentation algorithms based on deep learning can get a good result. At the same time, they require a large number of training samples [27]. Therefore, the application of deep learning algorithm in weed identification in the field was limited.

The adaptive integration of the color and texture attributes in the development of complex image descriptors is one of the most investigated topics of research in computer vision [28]. Montalvo *et al.* [29] successfully segmented maize crop from weeds using combinations of RGB color components derived from Principal Component Analysis (PCA). However, when the color difference between plants and weeds is not significant, inevitably other processes are needed, such as color space transformation [30]–[32]. Huang *et al.* [33] reported that land cover classification accuracy improved for the GeoEye-1 satellite imagery with an increase in intensity levels of traditional GLCMs, while for the QuickBird satellite it reduced from 91.5% to 90.3% with an increase in intensity levels. However, the effect of texture observes depends on some parameters. When using texture feature these parameters need to be optimized [34]. With the advantages of color features and texture features, the colortexture integration algorithm can be used to address complex segmentation problem [28], [35]–[38]. Sabzi *et al.* [39] used color and texture features for identifying weeds in order to perform site-specific spraying of herbicides. They used a neural network classifier combined with 126 color features and 60 texture features. The results showed that the segmentation accuracy was 98.38%. However, textures and colors of broccoli are different from maize. The classifier of the maize field cannot have excellent performance in a broccoli field. So it is necessary to select and optimize appropriate color and texture feature observer according to the characters of the broccoli field and develop an accurate classifier.

In this research, we considered the combination of color-texture features with an SVM to provide a discriminator to segment the broccoli seedling from soil and weeds. Such a segmentation operation calls the integration of several image processing approaches. Therefore the objectives of this research were:

1. To assess and optimize the capability of color features and texture features for discrimination of crops in a broccoli seedling field.

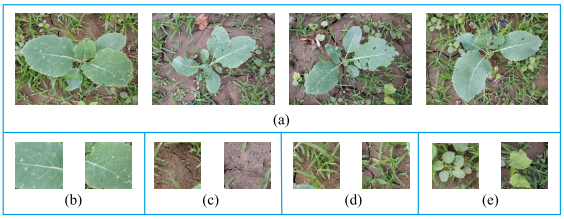

FIGURE 1. Sample images of the broccoli, soil and weeds from field data. (a) Original image (b)broccoli seedlings (c)Soil (d) Amaranthus retroflexus(AR) (e) Digitaria sanguinalis(DS).

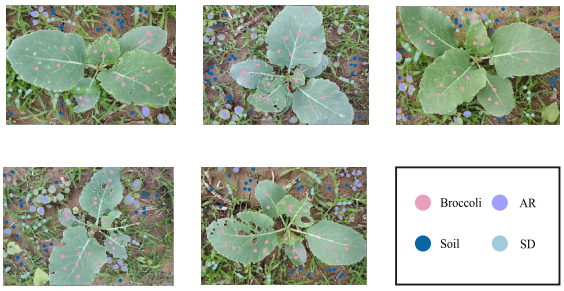

FIGURE 2. Images for algorithm development and pixels of broccoli, soil, AR and SD.

2. To develop a broccoli seedling segmentation algorithm based on classifier and noise removal method.

II. MATERIALS AND METHODS

A. IMAGE PREPARATION

Broccoli seedlings were grown on March 25, 2018 and transplanted on April 28, 2018. Images were taken from 10:00 to 12:00 on May 23, 2018 at the Beijing International Urban Agricultural Science and Technology Park, Beijing, China(116° 47' 57" E, 39°52' 7" N). The camera was Canon PowerShot SX150 IS, with the original resolution of 4032×3016. The results of this study would be run on a weeding machine.The algorithm would run on raspberry PI or minibox. So it was needed to limit the computational resources that the algorithm consumes. Image resolution was reduced to 400×300 to reduce the computational resources. Broccoli seedlings were aimed to be segmentated from two types of weeds (Amaranthus retroflexus and Digitaria sanguinalis) and soil. Fig 1 shows the broccoli seedlings, soil, Amaranthus retroflexus(AR) and Digitaria sanguinalis(DS).

In total, 105 images were provided. They were randomly divided into two groups. One group contained 55 images that were applied for algorithm development. The other group contained 50 images that were used for algorithm assessment.

Among 55 images used for algorithm development, 5 images were selected for classifier development and 50 for contour analyses and noise reduction. One hundred pixels of broccoli, soil, AR and SD were randomly selected from images for classifier development. In total 400 pixels were selected for classifier development. And they were randomly divided into a training set(300 samples) and a testing set(100 samples).The datasets used for algorithm development are presented in Fig 2.

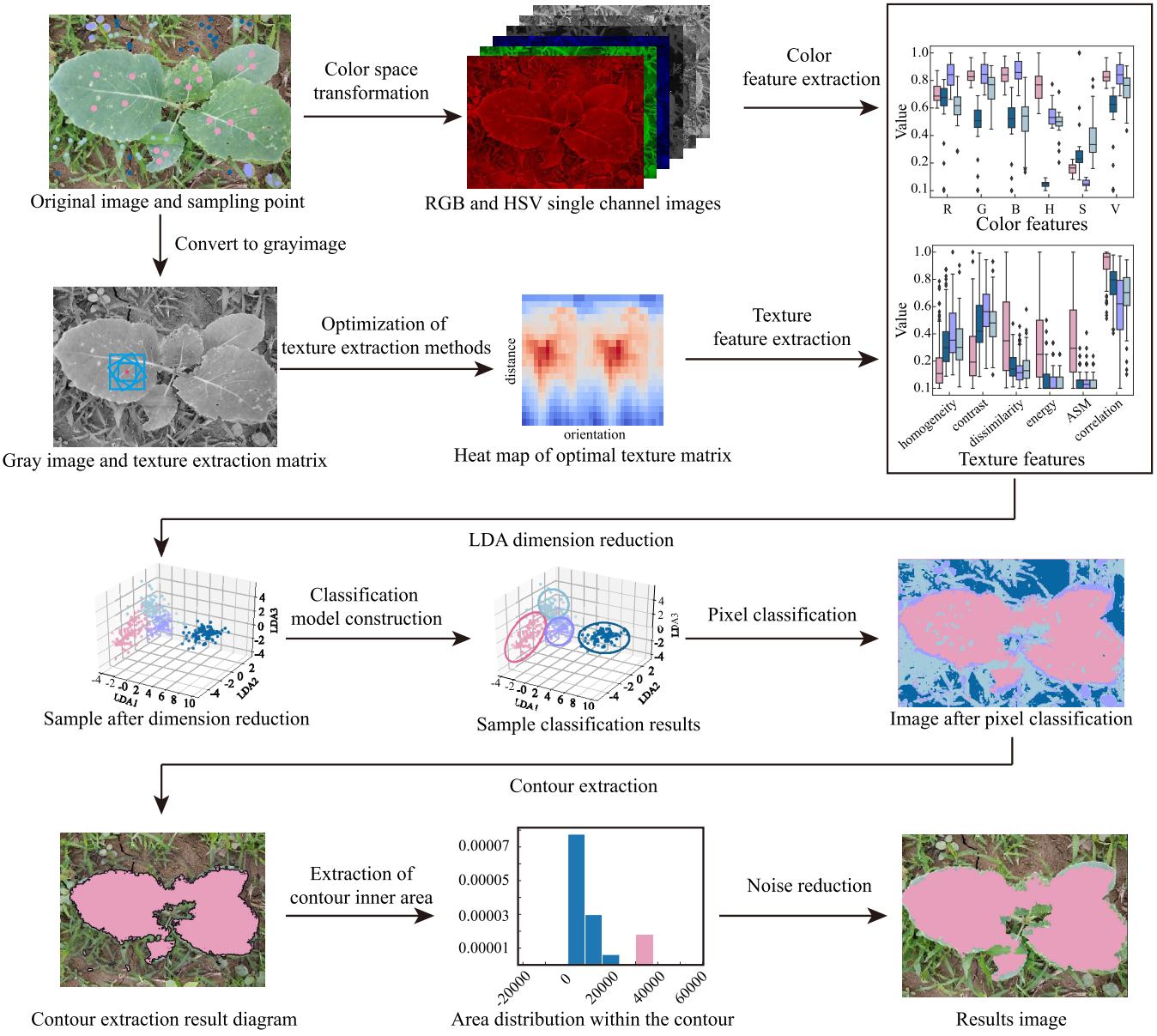

FIGURE 3. Segmentation algorithm.

B. GENERAL STEPS OF THE BROCCOLI SEGMENTATION ALGORITHM

The segmentation algorithm was composed of three general steps including: (1)color features selection and texture observers optimization;(2)pixels classifier based on SVM development, segmentation by pixel classification with SVM classifier; (3)noise removal. Fig 3 shows the summarised flowchart of image segmentation strategy using the proposed algorithm. OpenCVpyhon(3.4,2), numpy(1.13.3), scikitlearn(0.20.0), scikit image(0.13.0) were used to analyse the data.

C. EXTRACTION OF COLOR FEATURES

In this paper, a systematic experimentation was used to identify the acceptable color feature that best fits our broccoli segmentation algorithm. We employed a number of frequently used color spaces in our analysis, including RGB, HSV, XYZ, LAB, HED, YUV, YIQ color spaces. We utilized the gray-value of each raw channel of each color space as a color feature. In total, there were 21 color features obtained. They were R, G, B, H, S, V, X, Y, Z, L, A, B.1(the B channel of LAB color space), H.1(the H channel of HED color space), E, D, Y.1(the Y channel of YUV color space), U, V.1(the V channel of YUV color space),Y.2(the Y channel of YIQ color space), I, Q. After that, we used correlation analysis and chi-square tests to select effective features and redundant features. Pearson Correlation Coefficient(PCC) of each color feature groups combination was calculated. A chi-square test was used to analyze the correlation between features and classification target. When the PCC between two features was

higher than or equal to 0.8, the feature of high P-value from the chi-square test was deleted. The rest of the features was used for classifier development.

D. TEXTURE FEATURES EXTRACTION

The grey-level co-occurrence matrix (GLCM) is one of the most popular statistical approaches used in texture discrimination [40]. A unique co-occurrence matrix exists for each spatial relationship. The calculation of textures is dependent upon the direction(D) and the orientation(O) [41]. Therefore, we optimized D and O parameters of texture observer by grid search method. The search range of D was [0,19] and O was [0,360]° (resolution is 10°). The GLCM is quite complex, and some characteristic values of texture features are usually used as texture features. In this paper, characteristic values used include contrast, dissimilarity, homogeneity, ASM, energy, correlation. The calculation formulas are shown in (1)-(6). After texture features extraction, we also used Correlation Coefficient analyses and the chi-square test to select effective features.

$$Contrast = \sum_{i,j=0}^{levels-1} P_{i,j}(i-j)^2 \tag{1}$$

$$Dissimilarity = \sum_{i,j=0}^{levels-1} P_{i,j}|i-j| \tag{2}$$

$$Homogeneity = \sum_{i,j=0}^{levels-1} \frac{P_{i,j}}{1+(i-j)^2} \tag{3}$$

$$ASM = \sum_{i,j=0}^{levels-1} P_{i,j}^2 \tag{4}$$

$$Energy = \sqrt{ASM} \tag{5}$$

$$Correlation = \sum_{i,j=0}^{levels-1} P_{i,j}\left[\frac{(i-u_i)\left(j-u_j\right)}{\sqrt{(\sigma_i^2)(\sigma_j^2)}}\right] \tag{6}$$

where i is the row number; j is the column number; Pi,j is the normalized value in the cell i, j; N is the number of rows or columns.

E. DATA NORMALIZATION AND DATA REDUCTION

The data after normalization would be scaled to a reasonable range, and transferred to a non-dimensional data. As features extracted in this paper contained multiple dimensions and were not steady. Normalization formula was used for standardization to ensure that each dimension of the data ranges from zero to one [42]. Data normalization was calculated by (7).

$$y = \frac{x - x_{min}}{x_{max} - x_{min}} \tag{7}$$

where y is the normalized value, x is the original value, x_{min} is the minimum value and x_{max} is the maximum value.

Selected features contained both useful and irrelevant information for the broccoli seedlings identification. Also, it was necessary to do dimensionality reduction in order to quantitatively analyze features of broccoli seedlings and others [41]. Linear Discriminant Analysis(LDA) algorithm is a supervised dimensionality reduction algorithm, mainly taking categories as consideration factors to make the projected samples data as separable as possible [43]. Number of components is no more than the number of classes and the number of features ($n_{components} <= min(n_{classes}-1, n_{features})$) In order to retain more information while dimension reduction, we selected 3 as the number of components.

F. CLASSIFIER AND IMAGE PREPROCESSING

Classification is one of the main components of a segmentation algorithm. For this reason, the classifier should be selected carefully [39]. In this research, the support vector machine (SVM) was used for classifying the feature vectors into the 4 existing classes. Radial basis function (RBF) was adopted in the SVM classification model. When training an SVM with the RBF kernel, two parameters must be considered: C and gamma. The gamma parameter was 1/n_feature and C parameter was 1.0 based on the recommendation of the official document [44].

To find the minimum number of training samples, we searched the minimum number of training samples from 10 to 300 with a step size of 10. And the accuracy of the training set and testing set was calculated respectively to test the effect of classifier and avoid over-fitting. The accuracy calculation method is shown in (8). One hundred test samples were used to verify the classifier performance. Some indicators were used to evaluate classifier performance, includeing precision, pecall, f1-scores. The calculation formulas were shown in (9), (10), (11).

$$\text{Accuracy} = \frac{(TP+TN)}{(TP+FP+TN+FN)} \tag{8}$$

$$\text{Precision} = \frac{\text{TP}}{(\text{TP}+\text{FP})} \tag{9}$$

$$\text{Recall} = \frac{\text{TP}}{(\text{TP}+\text{FN})} \tag{10}$$

$$\text{F1}-\text{score} = \frac{(2\text{Recall} \times \text{Precision})}{(\text{Recall} + \text{Precision})} \tag{11}$$

where True Positive (TP) is the number of pixels detected as broccoli seedlings correctly. True Negative (TN) corresponds to the number of pixels detected as others correctly. False Positive (FP), the number of other pixels detected as broccoli seedlings and False Negative (FN), the number of broccoli seedlings pixels detected as others.

The classifier was used to classify every pixel in the image. We got the original segmentation result by the classification. There were some false broccoli seedling pixels in the original result, because of the error of the classifier. There were noises need to be removed. We removed noise by contour analysis. Fifty broccoli seedling contours and 50 false-broccoli seedling contours were manually labeled. The number of pixels in the contour was taken as the contour area, and the areas of broccoli seedling contours and false-broccoli

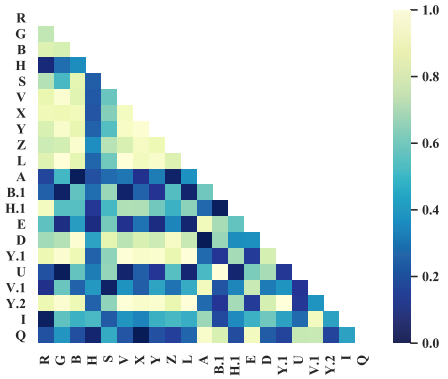

FIGURE 4. Color feature correlation matrix heat map.

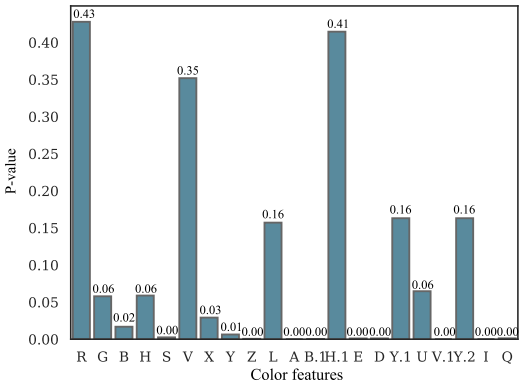

FIGURE 5. P-value bar chart of the color selection chi-test result.

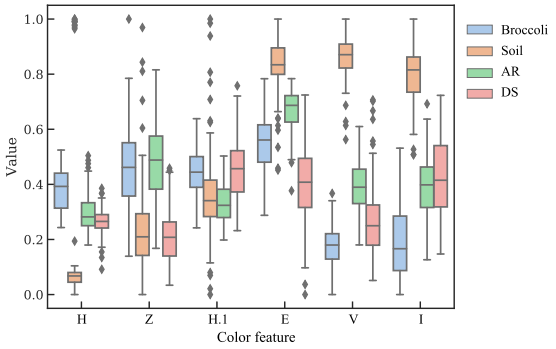

FIGURE 6. Boxplot of selected color features.

seedling contours were calculated. We used the threshold to remove the false-broccoli seedling contours. The threshold was the midpoint of the maximum false-broccoli seedling contour area and the minimum broccoli contour area.

III. RESULTS AND DISSCUSSION

A. COLOR FEATURE

By observing the correlation matrix heat map (Fig 4), the features with a correlation coefficient greater than 0.8 were divided into one group. In total, there were 6 groups. The first group was R, G, B, S V, X, Y, Z, A, D, Y.1, Q. The second group was the H channel. The correlation coefficient between H feature and any other features in this study was nothing more than 0.8. The third group was L, E, Q. The fourth group was B.1 and U. The fifth group was H.1. The sixth group was V.1 and I.

Due to the fact that color spaces could be converted by mathematical transformation, and the transformation relationship between some color channels was linear transformation, the Pearson correlation coefficient between these color features was high, and the information contained in the two types of features had repeated parts, which would generate redundant data and increase the computational burden. Highly correlated feature combinations were found through correlation analysis. The removal of the feature with a low correlation with the target problem in the combination could effectively improve the computational efficiency, but it would also cause a certain degree of information loss.

The chi-square test P-value of color features is shown in Fig 5. The lowest P-value of color features in first group was Z (2.43×10^{-7}), in the second group, was H (0.06), in the third group was E (9.90×10^{-4}), in the fourth group was V(7.38×10^{-14}), in the fifth group was H.1(0.41), and in the sixth group was I (7.38×10^{-14}).After correlation analysis and chi-square test, the color features for broccoli segmentation were H, Z, H.1, E, V and I. After the correlation analysis and chi-square test, the screened boxplot of color features is shown in Fig 6.

It can be seen from the Fig 6 that the mean value of soil in channel H was far away from the mean value of the other three types of targets, with less overlap, indicating that channel H could effectively distinguish soil from the other three types of targets; In the Z channel, the mean distance between broccoli and AR and the mean distance between soil and DS was large, indicating that Z channel could distinguish broccoli and AR from soil and DS. The mean distance of all targets in the H.1 channel was relatively close, and the discrimination ability was poor. This result was consistent with the results of the chi-square distribution test which was not significant, indicating that this channel contains information that other channels do not contain, but this information could not be effectively used in the classification of this study. All the mean values of the E channel were far away from each other, indicating that the channel had a superior ability to distinguish 4 types of targets. The mean values of the V channel and I channel were far from the other three types of targets, and the mean values of the other three types were close, indicating that these two channels had a strong ability to distinguish soil. Among the six selected color features, more color features can better distinguish soil from other three types of targets, while there were fewer features that could distinguish broccoli, AR and DS, indicating that color features could better distinguish vegetation from the soil, but the ability to distinguish green vegetation was weak.

B. TEXTURE FEATURE

Chi-square test results of texture features extracted from GLCM of different distance and orientation are shown in 7, and the minimum value of P-value and the position of the

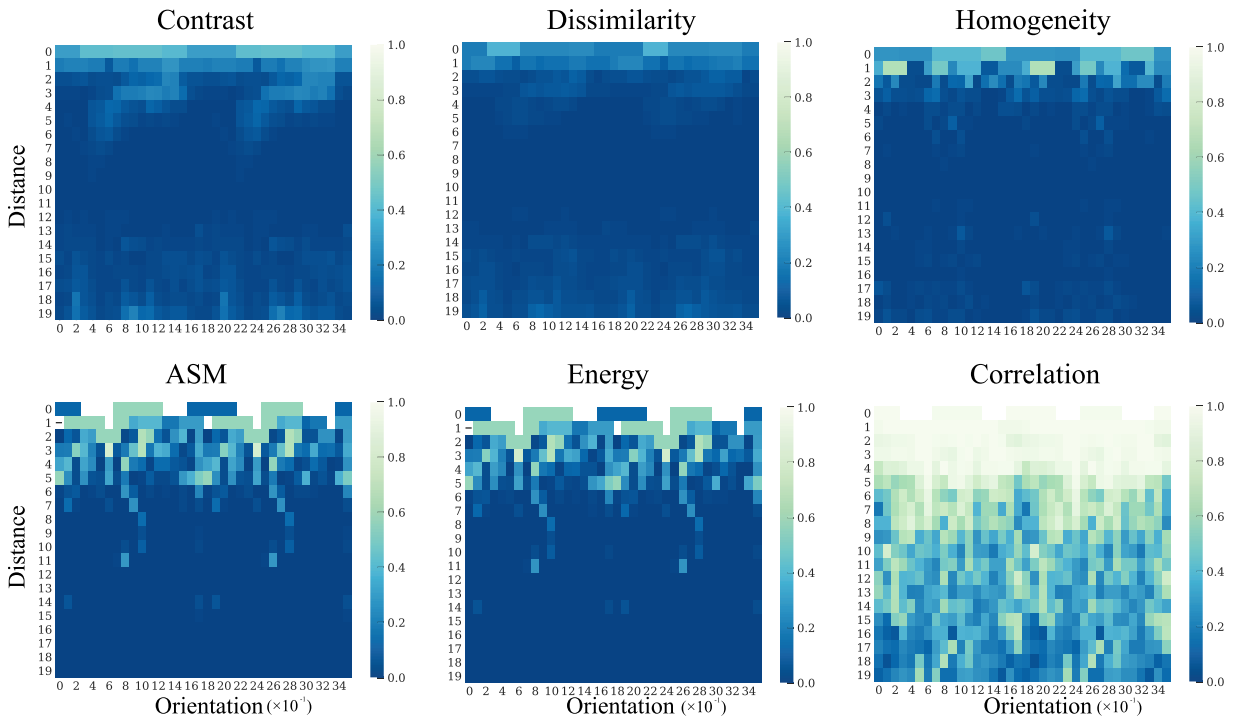

FIGURE 7. Heat map of texture optimization result.

TABLE 1. Texture feature chi - square test minimum value and location.

Features	Minimum P-value	Location
Dissimilarity	3.98×10^{-4}	(5,2),(5,20)
Homogeneity	2.25×10^{-6}	(9,12),(9,30)
ASM	1.16×10^{-10}	(19,4),(19,22)
Energy	8.19×10^{-11}	(19,4),(19,22)
Correlation	4.90×10^{-3}	(19,1),(19,19)

minimum value was shown in Table 1. Contrast, dissimilarity, homogeneity, ASM, energy and correlation minimum P-value were all lower than 0.05, which can significantly distinguish the target. There were two minimum points of P-value in the chi-square test of all texture features. We used Contrast, dissimilarity, homogeneity, ASM, energy as texture features, and the distances and orientation of each feature were (8,9), (5,2), (9,12), (19,4), (19,4) and (19,1).

The minimum P-value of the ASM, energy and correlation occurred when the distance was the maximum 19. It could be observed in the heat map that the P-value decreased with the increase of the distance in the interval of [0, 19]. Due to the limitation of computing resources in this study, the maximum value of the distance was 19. The distance of the minimum P-values of contrast, dissimilarity and homogeneity were all smaller than 19, indicating that there was a locally optimal solution in the interval of [0, 19].

By observing the heat map (Fig 7), it could be found that the heat map shows a repetition of π cycles, indicating that the features extracted by the gray symbiosis matrix of O and O + π were the same when extracting each texture feature. Therefore, an interval of π length could be chosen

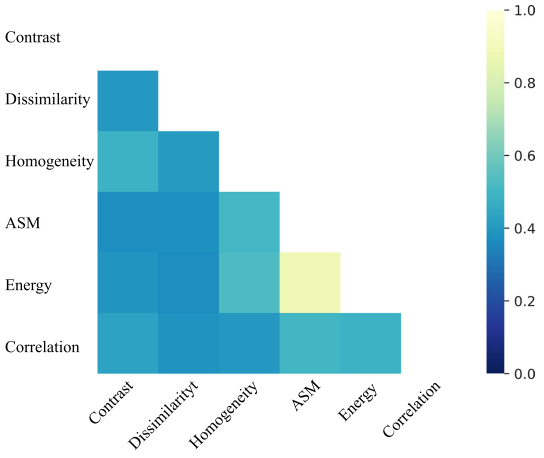

FIGURE 8. Correlation matrix heat map of texture features.

for optimization when seeking the optimal feature extraction matrix direction.

Results of texture feature correlation analysis are shown in Fig 8. The correlation between the ASM and energy was more than 0.8, showing a higher similarity, while the P-value of energy was smaller. The correlation coefficient between other features was no more than 0.8, indicating that the texture features contained less repeated information and had a strong correlation with the target problem.

The boxplot diagram of color features after chi-square test optimization and correlation analysis is shown in Fig 9. It could be seen from Fig 9 that the mean value of broccoli in each texture feature was far from the mean value of the other

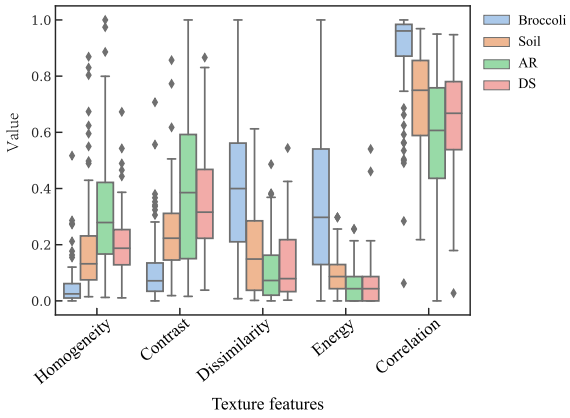

FIGURE 9. Boxplot of selected texture features.

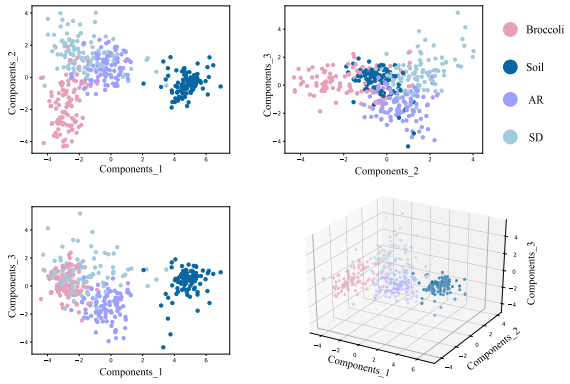

FIGURE 10. Feature distribution after dimension reduction by LDA.

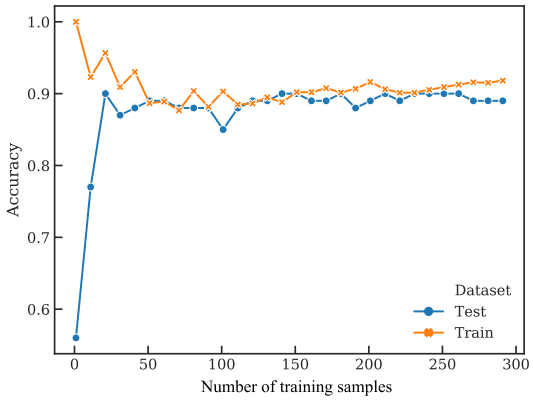

FIGURE 11. Relationship between the number of training samples and accuracy.

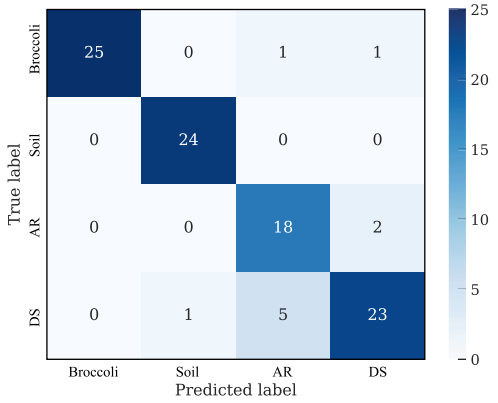

FIGURE 12. Confusion matrix heat map of the test set.

three types of targets, but the mean value of the other three types of targets was close to each other, so the texture feature had a good ability to distinguish broccoli, but a poor ability to distinguish the other three types of targets. The area of soil, AR and DS were relatively small. Due to the limitation of computing resources, the resolution of the images adopted in this study was too low to effectively extract the texture information of these features, which made the texture information unable to effectively distinguish AR and DS.

C. RESULTS OF CLASSIFICATION

Sample distribution after dimension reduction analysis of LDA is shown in Fig 10. It could be observed in the figure that the soil pixel was far away from the other three types of targets in the principal component space, which was easy to be classified. Broccoli, AR and DS were close to each other in the feature space, but the distribution centers did not overlap. Therefore, the kernel function of the classification model in this paper was RBF kernel function with satisfactory performance for linear inseparability problem.

The relationship between accuracy and the number of training samples was shown in Fig 11. After the number of samples was more than 50, the sample accuracy of the training set and test set gradually tended to be stable. They tended to be equal to each other, and not over-fitting occured. When the sample size was lower than 30, the accuracy of the test set increases rapidly, while the training set showed a decreasing trend. It indicated that the model training was not sufficient, and the sample number of the training set was small. When the sample size was within the range of [30,50], the accuracy of the test set and training set tended to be stable, but the accuracy of the training set was higher than that of the test set, which resulted in the over-fitting phenomenon and insufficient training samples. Therefore the best training sample size was 50.

The test set classification results confusion matrix is shown in Fig 12. Two of the 27 broccoli samples were identified as AR and DS, respectively. All the soil samples were accurately identified; two samples of AR were identified as DS, one sample of DS was identified as soil, and five samples were identified as AR. Since the color of weeds and broccoli was similar, and the leaves of AR and DS were small, the image resolution adopted in this paper was low, and it was difficult to effectively collect the texture information of weeds. Therefore, there were numerous errors in weed discrimination.

The evaluation results of the discriminant model were shown in Table 2, in which the precision of broccoli was the highest and the recall rate was 0.93, indicating that all broccoli samples identified by the model were correct, but some broccoli samples were identified as other samples.

TABLE 2. Texture feature chi - square test minimum value and location.

	Precision	Recall	F1-score
Broccoli	1.00	0.93	0.96
Soil	0.96	1.00	0.98
AR	0.75	0.90	0.82
DS	0.88	0.79	0.84

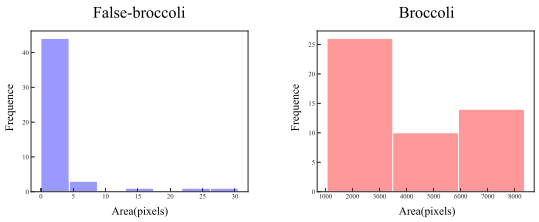

FIGURE 13. Statistical results of contour area.

The precision of soil was lower than 0.96, and the recall rate was higher than 1, indicating that all soil samples were correctly identified, but some other samples were identified as soil samples. The precision and recall rate of AR and DS was lower than those of soil and broccoli, indicating that the discriminant model had a poor discriminatory effect on weeds. Among them, the precision of AR was low and the recall rate was high, indicating that more false-AR samples were identified as AR. The high precision and low recall rate of DS indicate that more DS samples precision judged as other samples.

D. CONTOUR AREA

Statistical results of broccoli seedling contour area and false-broccoli seedling area are shown in Fig 13. False-broccoli seedling contour pixels were mainly concentrated in the interval of [0, 30], with the maximum not exceeding 30, while the broccoli seedling contour area was in the interval of [1000, 35000], with the minimum value not less than 1000. The segmentation point value was 515. The broccoli seedling contours and false-broccoli seedling contours had a significant difference in area, so it is easy to remove noise from the contour area.

E. FINAL RESULT

Pixel classification results and broccoli contour extraction results are shown in Fig 14.The regression analysis results are shown in Fig 15. Determination coefficient R^2 was 0.91, indicating that there was a strong linear correlation between ground truth results and algorithm segmentation results. The root mean square error was 0.10, indicating that the error was small. The slope k of the regression equation was 1.06, indicating that the pixel points recognized by the algorithm were less than those manually marked. Observing Fig 15, it could be found that the broccoli pixels at the edge of the leaf were not recognized. When extracting texture pixel points at the edge of the leaf, other pixel points were extracted, which leads to the incorrect classification of pixel points at the edge of the leaf.

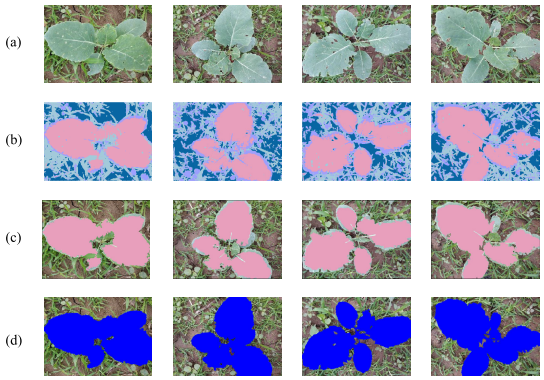

FIGURE 14. Result images: (a)original images; (b)classification results; (c)final results; (d)ground-truth.

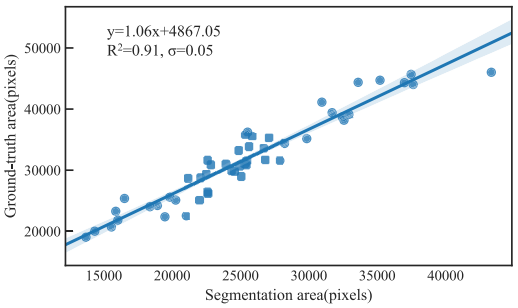

FIGURE 15. The area regression analysis result between ground-truth and segmentation result.

F. DISSCUSSION

In this paper, we developed a broccoli seedling segmentation method. We find efficient color features and texture feature that could be used to identify broccoli seedlings. Broccoli seedling had a significant difference in color with soil. It was easy to segment crops and soil in the field. But it was hard to segment objects with color features in images that object and background were close in color. Color space transfer could help us get more color features. Some color features could be obtained by color space transfer. But there was too much redundant information. It was necessary to selected efficient color features. In addition to color features, texture features could also be used to distinguish crops and weeds. The distance and orientation had a significant effect on the texture features.

Deep learning is a kind of new algorithm. It was widely used in image segmentation and always got a good result. But image segmentation based on deep learning usually requires several thousands of training samples. The labels for images segmentation task is hard to make. It takes a lot of labor and material resources. The algorithm was designed for weeding robots. It would be used on a Raspberry Pi or a Minibox. So it is necessary to consider the limitation of computer resources. So we developed the segmentation method in this paper. It only requires 300 pixels as training samples. It saves a lot of labor and easy to train.

IV. CONCLUSION

In this paper, broccoli field images were gathered by a camera. Color features and texture features were extracted. And pixels were classified by the support vector machine algorithm. Noise pixel points were eliminated by the contour area, and the segmentation and extraction of broccoli in a field environment were achieved. Through the analysis of the experimental results, it was found that:

(1) Color features could effectively distinguish soil from vegetation, while texture features could effectively distinguish different vegetations;

(2) The classification algorithm based on SVM could use fewer samples to obtain a higher classification accuracy. After dimension reduction by the LDA algorithm, the SVM algorithm was adopted to classify pixel points. When the training sample is greater than 50, the accuracy of the test set could reach 90%.

(3) Image segmentation can be done through pixel classification. The determination coefficient of the extracted broccoli area by the algorithm and the manually extracted broccoli area was 0.91, and the root-mean-square error was 0.1.

(4) The broccoli image segmentation model established by pixel classification could effectively segment broccoli images in the field environment with fewer training samples.

REFERENCES

[1] J. Mcmurray, "The origin, distribution and classification of cultivated broccoli varieties," *SEG Tech. Program Expanded Abstr.*, vol. 52, no. 9, pp. 76–80, 1999.

[2] M. Shahbandeh. *Global Production of Vegetables in 2017, by Type (in Million Metric Tons)*. Accessed: Jan. 28, 2019. [Online]. Available: https://www.statista.com/statistics/264065/global-production-of-vegetables-by-type/

[3] E. T. L. van Bueren, S. S. Jones, L. Tamm, K. M. Murphy, J. R. Myers, C. Leifert, and M. M. Messmer, "The need to breed crop varieties suitable for organic farming, using wheat, tomato and broccoli as examples: A review," *NJAS-Wageningen J. Life Sci.*, vol. 58, nos. 3–4, pp. 193–205, 2011.

[4] C. Andreasen and H. Stryhn, "Increasing weed flora in Danish beet, pea and winter barley fields," *Crop Protection*, vol. 36, no. 3, pp. 11–17, 2012.

[5] P. G. Kughur, "The effects of herbicides on crop production and environment in Makurdi Local Government Area of Benue State, Nigeria," *J. Sustain. Develop. Afr.*, vol. 14, no. 4, pp. 433–456, 2012.

[6] S. Christensen, H. T. Søgaard, P. Kudsk, M. Nørremark, I. Lund, E. S. Nadimi, and R. N. Jørgensen, "Site-specific weed control technologies," *Weed Res.*, vol. 49, no. 3, pp. 233–241, 2009.

[7] A. Bakhshipour, A. Jafari, S. M. Nassiri, and D. Zare, "Weed segmentation using texture features extracted from wavelet sub-images," *Biosyst. Eng.*, vol. 157, pp. 1–12, May 2017.

[8] R. Kamath, M. Balachandra, and S. Prabhu, "Raspberry Pi as visual sensor nodes in precision agriculture: A study," *IEEE Access*, vol. 7, pp. 45110–45122, 2019.

[9] D. Stroppiana, P. Villa, G. Sona, G. Ronchetti, G. Candiani, M. Pepe, L. Busetto, M. Migliazzi, and M. Boschetti, "Early season weed mapping in rice crops using multi-spectral UAV data," *Int. J. Remote Sens.*, vol. 39, nos. 15–16, pp. 5432–5452, 2018.

[10] M. J. Khan, H. S. Khan, A. Yousaf, K. Khurshid, and A. Abbas, "Modern trends in hyperspectral image analysis: A review," *IEEE Access*, vol. 6, pp. 14118–14129, 2018.

[11] C. Lammie, A. Olsen, T. Carrick, and M. R. Azghadi, "Low-power and high-speed deep FPGA inference engines for weed classification at the edge," *IEEE Access*, vol. 7, pp. 51171–51184, 2019.

[12] W. Kazmi, F. Garcia-Ruiz, J. Nielsen, J. Rasmussen, and H. J. Andersen, "Exploiting affine invariant regions and leaf edge shapes for weed detection," *Comput. Electron. Agricult.*, vol. 118, pp. 290–299, Oct. 2015.

[13] L. Ge, Z. Yang, Z. Sun, G. Zhang, M. Zhang, K. Zhang, C. Zhang, Y. Tan, and W. Li, "A method for broccoli seedling recognition in natural environment based on binocular stereo vision and Gaussian mixture model," *Sensors*, vol. 19, no. 5, p. 1132, 2019.

[14] G. Alenya, B. Dellen, S. Foix, and C. Torras, "Robotized plant probing: Leaf segmentation utilizing time-of-flight data," *IEEE Robot. Autom. Mag.*, vol. 20, no. 3, pp. 50–59, Sep. 2013.

[15] K. Kusumam, T. Krajník, S. Pearson, T. Duckett, and G. Cielniak, "3D-vision based detection, localization, and sizing of broccoli heads in the field," *J. Field Robot.*, vol. 34, no. 8, pp. 1505–1518, 2017.

[16] W. Kazmi, S. Foix, G. Alenyà, and H. J. Andersen, "Indoor and outdoor depth imaging of leaves with time-of-flight and stereo vision sensors: Analysis and comparison," *ISPRS J. Photogram. Remote Sens.*, vol. 88, pp. 128–146, Feb. 2014.

[17] A. Krizhevsky, I. Sutskever, and G. E. Hinton, "ImageNet classification with deep convolutional neural networks," *Commun. ACM*, vol. 60, no. 2, pp. 84–90, Jun. 2012.

[18] J. Long, E. Shelhamer, and T. Darrell, "Fully convolutional networks for semantic segmentation," in *Proc. IEEE Conf. Comput. Vis. Pattern Recognit. (CVPR)*, Jun. 2015, pp. 3431–3440.

[19] F. Yu and V. Koltun, "Multi-scale context aggregation by dilated convolutions," 2015, *arXiv:1511.07122*. [Online]. Available: https://arxiv.org/abs/1511.07122

[20] C. Peng, X. Zhang, G. Yu, G. Luo, and J. Sun, "Large kernel matters—Improve semantic segmentation by global convolutional network," 2017, *arXiv:1703.02719*. [Online]. Available: https://arxiv.org/abs/1703.02719

[21] B.-F. Wu and C.-H. Lin, "Adaptive feature mapping for customizing deep learning based facial expression recognition model," *IEEE Access*, vol. 6, pp. 12451–12461, 2018.

[22] X. Zhang, Y. Qiao, F. Meng, C. Fan, and M. Zhang, "Identification of maize leaf diseases using improved deep convolutional neural networks," *IEEE Access*, vol. 6, pp. 30370–30377, 2018.

[23] A. Farooq, J. Hu, and X. Jia, "Analysis of spectral bands and spatial resolutions for weed classification via deep convolutional neural network," *IEEE Geosci. Remote Sens. Lett.*, vol. 16, no. 2, pp. 183–187, Feb. 2018.

[24] N. Teimouri, M. Dyrmann, P. R. Nielsen, S. K. Mathiassen, G. J. Somerville, and R. N. Jørgensen, "Weed growth stage estimator using deep convolutional neural networks," *Sensors*, vol. 18, no. 5, p. 1580, 2018.

[25] H. Huang, J. Deng, Y. Lan, A. Yang, X. Deng, and L. Zhang, "A fully convolutional network for weed mapping of unmanned aerial vehicle (UAV) imagery," *PLoS ONE*, vol. 13, no. 4, 2018, Art. no. e0196302.

[26] X. Ma, X. Deng, L. Qi, Y. Jiang, H. Li, Y. Wang, and X. Xing, "Fully convolutional network for rice seedling and weed image segmentation at the seedling stage in paddy fields," *PLoS ONE*, vol. 14, no. 4, 2019, Art. no. e0215676.

[27] F. Ghasemi, A. Mehridehnavi, A. Pérez-Garrido, and H. Pérez-Sánchez, "Neural network and deep-learning algorithms used in QSAR studies: Merits and drawbacks," *Drug Discovery Today*, vol. 23, no. 10, p. 1784, 2018.

[28] D. E. Ilea and P. F. Whelan, "Image segmentation based on the integration of colour–texture descriptors—A review," *Pattern Recognit.*, vol. 44, nos. 10–11, pp. 2479–2501, 2011.

[29] M. Montalvo, M. Guijarro, J. M. Guerrero, and A. Ribeiro, "Identification of plant textures in agricultural images by principal component analysis," in *Proc. Int. Conf. Hybrid Artif. Intell. Syst.*, 2016, pp. 391–401.

[30] Z. Tufail, K. Khurshid, A. Salman, I. F. Nizami, K. Khurshid, and B. Jeon, "Improved dark channel prior for image defogging using RGB and YCbCr color space," *IEEE Access*, vol. 6, pp. 32576–32587, 2018.

[31] T. Zhang, H.-M. Hu, and B. Li, "A naturalness preserved fast dehazing algorithm using HSV color space," *IEEE Access*, vol. 6, pp. 10644–10649, 2018.

[32] S. Y. Kahu and K. M. Bhurchandi, "A low-complexity, sequential video compression scheme using frame differential directional filter bank decomposition in CIE La^* b^* color space," *IEEE Access*, vol. 5, pp. 14914–14929, 2017.

[33] X. Huang, X. Liu, and L. Zhang, "A multichannel gray level co-occurrence matrix for multi/hyperspectral image texture representation," *Remote Sens.*, vol. 6, no. 9, pp. 8424–8445, 2014.

[34] T. U. Rehman, Q. U. Zaman, Y. K. Chang, A. W. Schumann, K. W. Corscadden, and T. J. Esau, "Optimising the parameters influencing performance and weed (goldenrod) identification accuracy of colour co-occurrence matrices," *Biosyst. Eng.*, vol. 170, pp. 85–95, Jun. 2018.

[35] Y. Dong, H. Zhang, Z. Liu, C. Yang, G.-S. Xie, L. Zheng, and L. Wang, "Neutrosophic set transformation matrix factorization based active contours for color texture segmentation," *IEEE Access*, vol. 7, pp. 93887–93897, 2019.
[36] Y. Akbulut, Y. Guo, and A. Şengür, and M. Aslan, "An effective color texture image segmentation algorithm based on hermite transform," *Appl. Soft Comput.*, vol. 67, pp. 494–504, Jun. 2018.
[37] M. Kiechle, M. Storath, A. Weinmann, and M. Kleinsteuber, "Model-based learning of local image features for unsupervised texture segmentation," *IEEE Trans. Image Process.*, vol. 27, no. 4, pp. 1994–2007, Apr. 2018.
[38] L. F. S. Scabini, R. H. M. Condori, W. N. Gonçalves, and O. M. Bruno, "Multilayer complex network descriptors for color–texture characterization," *Inf. Sci.*, vol. 491, pp. 30–47, Jul. 2019.
[39] S. Sabzi, Y. Abbaspour-Gilandeh, and G. García-Mateos, "A fast and accurate expert system for weed identification in potato crops using metaheuristic algorithms," *Comput. Ind.*, vol. 98, pp. 80–89, Jun. 2018.
[40] R. M. Haralick, "Statistical and structural approaches to texture," *Proc. IEEE*, vol. 67, no. 5, pp. 786–804, May 1979.
[41] F. Lin, D. Zhang, Y. Huang, X. Wang, and X. Chen, "Detection of corn and weed species by the combination of spectral, shape and textural features," *Sustainability*, vol. 9, no. 8, p. 1335, 2017.
[42] N. Nakanishi, "Normalization condition and normal and abnormal solutions of the Bethe–Salpeter equation," *Phys. Rev.*, vol. 138, no. 5B, p. B1182, 1965.
[43] J. Wen, X. Fang, J. Cui, L. Fei, K. Yan, Y. Chen, and Y. Xu, "Robust sparse linear discriminant analysis," *IEEE Trans. Circuits Syst. Video Technol.*, vol. 29, no. 2, pp. 390–403, Feb. 2019.
[44] Scikit-Learn v0.21.3. *Support Vector Machines*. Accessed: Sep. 10, 2019. [Online]. Available: https://scikit-learn.org/stable/modules/svm.html

KUNLIN ZOU received the B.E. degree in mechatronic engineering from Tarim University, Xinjiang, China, in 2016, and the master's degree in mechatronic engineering from Shihezi University, China. He is currently pursuing the Ph.D. degree with China Agricultural University, China. His current research interests are face digital image processing and artificial intelligent.

LUZHEN GE received the B.E. degree in mechanical design and manufacturing and automation from Liaocheng University, Shandong, China, in 2014, and the master's degree in mechanical manufacturing and automation from China Agricultural University, Beijing, China, in 2016, where he is currently pursuing the Ph.D. degree. His current research interests are deep learning, pattern recognition, and stereo vision.

CHUNLONG ZHANG received the B.E. and Ph.D. degrees in mechanical engineering from China Agricultural University, in 2009 and 2014, respectively. From 2012 to 2013, he was a Visiting Scholar with the Robotics Institute, Carnegie Mellon University. He is currently an Associate Professor with the College of Engineering, China Agricultural University. His main research interests include machine vision and agricultural robotics.

TING YUAN was born in Zhoushan, Zhejiang, China, in 1981. He received the B.S. and Ph.D. degrees in mechanical engineering from China Agricultural University, in 2004 and 2012, respectively. From 2012 to 2016, he was a Lecturer with the Agricultural Robot Laboratory. Since 2017, he has been an Associate Professor with the Department of Mechanical Design and Manufacturing, College of Engineering, China Agricultural University. He is the author of one book, more than 20 articles, and more than 20 inventions. His research interests include machine vision, agricultural robot, and intelligent agricultural equipment.

WEI LI received the B.E. degree in mechanical design and manufacturing and automation from Jilin University, Jilin, China, in 1982, and the Ph.D. degree in vehicle engineering from China Agricultural University, Beijing, China, in 2004. She is currently a Professor of mechanical engineering with China Agricultural University. Her research interests are intelligent agricultural equipment and robot. She has over 180 publications in these areas. She has undertaken more than 20 projects in the field of modern agriculture of China, including the National Science and Technology Support Program, the National 863 Program, the National Natural Science Foundation, and the National Key Research and Development Program.